ELSEVIER

Journal of Chromatography A, 855 (1999) 349–366

JOURNAL OF CHROMATOGRAPHY A

www.elsevier.com/locate/chroma

Dynamics of capillary electrochromatography II. Comparison of column efficiency parameters in microscale high-performance liquid chromatography and capillary electrochromatography

E. Wen, R. Asiaie, Cs. Horváth*

Department of Chemical Engineering, Yale University, P.O. Box 208286, New Haven, CT 06520-8286, USA

Received 13 April 1999; received in revised form 18 May 1999; accepted 3 June 1999

Abstract

In capillary electrochromatography (CEC) the flow of the mobile phase is generated by electrosmotic means in high electric field. This work compares band spreading measured experimentally in several packed capillaries with electrosmotic flow (EOF) and viscous flow under otherwise identical conditions. The data were fitted to the simplified van Deemter equation for the theoretical plate height, $H = A + B/u + Cu$, in order to evaluate parameters A and C in each mode of flow in the different columns. The ratio of these two parameters obtained with the same column in microscale HPLC (μ-HPLC) and CEC was used to quantify the attenuation of their contribution to band spreading upon changing from viscous flow (in μ-HPLC) to electrosmotic flow (in CEC). The capillary columns used in this study were packed with stationary phases of different pore sizes as well as retentive properties and measurements were carried out under different mobile phase conditions to examine the effects of the retention factor and buffer concentration. In the CEC mode, the value of both column parameters A and C was invariably by a factor of two to four lower than in the μ-HPLC mode. This effect may be attributed to the peculiarities of the EOF flow profile in the interstitial space and to the generation of intraparticle EOF inside the porous particles of the column packing. Thus, band spreading due to flow maldistribution and mass transfer resistances is significantly lower when the mobile phase flow is driven by voltage as in CEC, rather than by pressure as in μ-HPLC.

Keywords: Electrochromatography; Efficiency; Band profiles

1. Introduction

Capillary electrochromatography (CEC) combines features of capillary zone electrophoresis (CZE) and microscale high-performance liquid chromatography (μ-HPLC). It employs a capillary column containing the stationary phase [1–4], which has fixed charges at the interface, and electrosmotic flow (EOF) of the mobile phase generated by high electric field. The separation of ionized sample components is determined by differences in both their retention on the stationary phase and by their electrophoretic mobility. The interest in CEC as an analytical separation technique stems, among others, from the possibility

*Corresponding author. Tel.: +1-203-432-4357; fax: +1-203-432-4360.

E-mail address: csaba.horvath@yale.edu (Cs. Horváth)

0021-9673/99/$ – see front matter
PII: S0021-9673(99)00705-0

of using relatively long packed capillary columns of low plate heights to obtain peak capacities significantly higher than those obtained in HPLC with viscous flow within the traditional limits on the permissible column inlet pressure [5–8]. So far CEC was mainly employed for the separation of neutral sample components under conditions similar to those of reversed-phase chromatography and the results have demonstrated that high peak efficiencies are indeed attainable with this liquid phase separation technique [9–13].

It has been postulated [14], and found experimentally in certain cases [5,7,15–17], that the magnitude of band spreading is lower with voltage– than with pressure-driven flow. The improvement was attributed mostly to relaxation of the band spreading effect of flow maldistribution in the interstitial space of packed columns due to the peculiarities of the electrosmotic flow. Only recently has been paid attention to augmentation of intraparticle mass transport by electrosmosis and to the concomitant attenuation of band spreading [18]. Nevertheless the comparison of the magnitude of band spreading with viscous flow (μ-HPLC) and with EOF (CEC) in a given column fell short so far of a methodical approach.

The present study is aimed at a systematic examination of band spreading in various packed capillary columns, each operated separately with viscous and electrosmotic flow of the mobile phase, under otherwise identical conditions. The comparison of the results is expected to shed light on the sources of efficiency enhancement when a given column is used with voltage- instead of pressure-driven mobile phase flow. Since the details of the thermodynamic, kinetic, and transport phenomena underlying the differential migration process in CEC are still poorly understood, we shall employ, for making such comparison, the experimentally evaluated parameters of the simplified van Deemter equation [19] and its variants [20–22]. Comparison of the corresponding parameters obtained with a given column in both the CEC and μ-HPLC modes under otherwise identical conditions offers a unique opportunity to gain insight into the factors which are responsible for the attenuation of band spreading when viscous flow is replaced by electrosmotic flow in a given column.

2. Experimental

2.1. Chemicals

Reagent grade monobasic sodium phosphate and dibasic sodium phosphate were purchased from J.T. Baker (Phillisburg, NJ, USA). HPLC-grade acetonitrile, methanol, acetone, and toluene were obtained from Fisher Scientific (Pittsburgh, PA, USA). Benzaldehyde, formamide and the polycyclic aromatic hydrocarbon samples: naphthalene, biphenyl, fluorene, fluoranthene, and *m*-terphenyl were supplied by ChemServices (West Chester, PA, USA). Acrylamide was obtained from American Bioanalytical (Natick, MA, USA). The water used throughout was purified and deionized with a Nanopure system (Barnstead, Boston, MA, USA).

A sodium phosphate stock solution was prepared by mixing 100 ml of 100 m*M* NaH_2PO_4 solution and 180 ml of 100 m*M* Na_2HPO_4. The 100 m*M* sodium phosphate solution, pH 7.0, thus obtained was diluted with water or with water and acetonitrile to prepare an aqueous or a hydro-organic buffer of the appropriate sodium phosphate concentration, respectively.

Polyimide clad fused-silica capillaries with either a 50 or 75 μm inner diameter and 375 μm outer diameter were purchased from Quadrex (New Haven, CT, USA). Zorbax octadecylated silica particles with 6 μm particle diameter and 80 Å or 300 Å mean pore diameter were complementary samples from Rockland Technologies (Newport, DE, USA). Gigaporous polystyrene divinyl benzene based strong cation exchangers having a particle diameter of 8 μm and a pore diameter of 1000 Å were a gift from Polymer Labs. (Church Stretton, UK). Samples of siliceous cation exchanger and octadecylated silica particles having a nominal particle size of 5 μm and pore diameter of 300 Å were donated by Phase Separations (Deeside, UK).

2.2. Stationary phases and column packing procedures

A slightly modified version of the packing procedure described before [3,7] was adapted for the

packing of siliceous and polymeric particles into fused-silica capillaries having I.D. of 50 or 75 μm. Fused silica capillaries of 400 mm length were tapped in a vial of 5 μm dry silica particles to fill a 0.2–0.3 mm long length. A Type 3A Blowpipe (Veriflo, Richmond, VA, USA) with oxygen–butane was used to make a packing frit by sintering the particles. The permeability and stability of the frit were tested at pressures up to 6000 p.s.i. with a constaMetric III (Thermo Separation Products, San Jose, CA, USA) metering pump. A 2% (w/v) slurry of octadecylated silica (ODS) particles was made in a 1:1 mixture of toluene and acetone. For packing columns with strong cation exchangers aqueous slurries were employed. In all cases, the slurry was placed in a cylindrical stainless steel reservoir (50× 2 mm) connected to the capillary. For octadecylated silica particles, methanol was used as the packing solvent, whereas water was used for the strong cation exchangers. The packing liquid was pumped through the reservoir by an Altex Model 100A pump (Beckman, Berkeley, CA, USA) at 400 bar until the packing reached at least 20 cm. Then the column was disconnected from the reservoir and attached directly to the pump. It was flushed with water at 150 bar and simultaneously at about 20 cm from the pump inlet, a frit was formed by sintering by using an electrically heated Ni–Cr wire looped around the capillary. Then the column was removed from the pump assembly, the packing frit was cut and the column was placed in the reverse direction to facilitate the removal of the packing after the outlet frit. After the extra packing was removed, a 2 mm wide detection window was made by electrically burning the polyimide coating. Finally, the inlet frit was made at the other end of the column, approximately 5 mm from the pump. With polymeric particles the column was allowed to pack for approximately 25 cm as described above. Then the pump was turned off and the pressure was allowed to decline slowly so that the packing is not disturbed by a sudden release of pressure. The packing reservoir was cleaned and refilled with 2 μm silica particles (Glycotech, Hamden, CT, USA). A further 5 mm silica was then packed and used to form the outlet retaining frit according to the procedure described above.

2.3. Instrumentation

2.3.1. μ-HPLC

All μ-HPLC experiments were performed on a modified Hewlett-Packard Model 1090 liquid chromatograph (Wilmington, DE, USA) equipped with a Model DRV 5 high-performance pumping system and an auto-injector. In order to operate the instrument in the flow-rate range required for capillary columns, the mobile phase flow was split after the injection valve by using a T fitting from Upchurch Scientific (Oak Harbor, WA, USA) and a restrictor capillary. The column was mounted at right angles to the fluid inlet of the T piece with the restrictor capillary placed opposite to the fluid inlet. Split ratios were typically in the order of 4000:1 and adjusted by altering the length and diameter of the restrictor capillary. A Thermo Separations Products Model UV 2000 (San Jose, CA, USA) dual wavelength UV–Vis detector with a Model 9550-0155 cell for on-column detection was placed in close proximity to the left hand side of the chromatograph at the same level as the injector valve setup in order to minimize the length of connecting tubing required. Data was collected using the DOS version 1.1 of the Hewlett-Packard ChemStation software, which was installed on a Hewlett-Packard Vectra 486DX33 IBM compatible computer running Windows 3.1 operating system. The UV detector was connected to the computer through a Model 35900 analog/digital interface by Hewlett-Packard.

Columns were connected directly into one end of the T piece and the detector position was adjusted so that the column effluent was monitored immediately after the retaining frit at the outlet, while keeping the column straight. After installation the column was flushed with the eluent at an inlet pressure of about 50 bar for 30–40 min until stable baseline was obtained at 200 nm. During data acquisition the absorbance was monitored at 200 nm. All μ-HPLC experiments were carried out at room temperature. The 10 μl samples injected before the split were of the same composition as those employed in the CEC experiments.

2.3.2. Capillary electrochromatography

The experiments were conducted with a Hewlett-

Packard Model HP[3D]CE capillary electrophoresis unit which was connected to a nitrogen cylinder to pressurize both the inlet and outlet vials up to 12 bar. A Model P150 Hewlett-Packard personal computer with ChemStation v. 4.01 application and Windows 95 (Microsoft, Redmond, WA, USA) installed was used to control the instrument functions and to acquire the data.

In the Model HP[3D]CE unit, the capillary column was equilibrated with the buffer solution according to a two step protocol. First, 12 bar nitrogen pressure was applied to the column inlet for 60 min. Second, the column was flushed electrokinetically at 15 kV for 60 min, while 12 bar nitrogen pressure was applied to both the inlet and outlet of the column. The same washing regimen was also employed each time after changing the running buffer. For each stationary phase/eluent combination a series of voltages were applied. All the CEC experiments were carried out at 25°C using a forced air thermostat. The analytes were injected electrokinetically at 10 kV for 1 s. The injected samples contained approximately 0.5 mg/ml of each eluate dissolved in the mobile phase. For each chromatogram the applied voltage, the current and UV absorbance, at 200 nm were recorded.

2.4. Data processing

In both the μ-HPLC and CEC experiments, the migration time (measured at the peak apex), peak area, peak height and width at half height were recorded. The data were analyzed using Excel v5.0 software (Microsoft) and the PeakFit v3.0 package (Jandel Scientific, Chicago, IL, USA) with a non-linear least-squares curve-fitting program was used to obtain the best fit.

In processing the data, the chromatographic velocity of the mobile phase, u [21] was used throughout. It was obtained from the migration time of acrylamide, which served as the inert tracer, divided by the packed length of the column, L. The number of theoretical plates, N, was calculated from the peak variance [23–25] evaluated from the peak width at half height as well as from the area and height of the peaks. The plate height, H, was obtained from the relationship $H = L/N$. The dimensionless (reduced) plate height, h, is calculated as H/d_p where d_p is the particle diameter of the column packing.

3. van Deemter analysis of column efficiency in μ-HPLC and CEC

In linear elution chromatography, band spreading in the column is traditionally measured by the 'plate height' and by the dimensionless 'plate number' [23–25] that express the variance per unit length of the column and the dimensionless peak variance, respectively. Many plate height equations have been introduced to relate the plate height to column properties and to operational variables. All of these equations are based on the additivity of the incremental variances arising from various independent contributions to band spreading [22,26].

In this work, we also assume [27] that the classical chromatographic model applies to CEC of small uncharged substances and use the simplified van Deemter equation [19] as follows,

$$H = A + \frac{B}{u} + Cu \qquad (1)$$

It is illustrated in Fig. 1 by plots of the plate height and the three terms of Eq. (1), representing the corresponding plate height increments, against the mobile phase velocity. The first term, A, of the

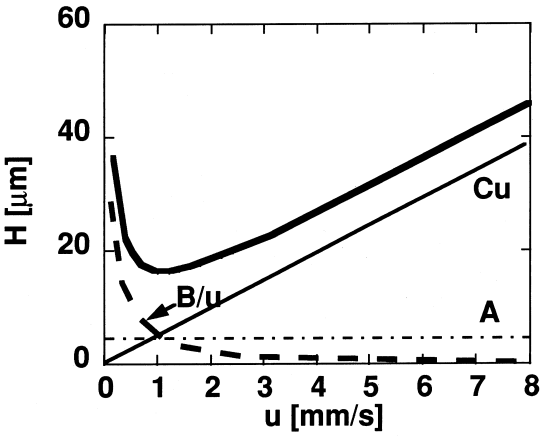

Fig. 1. van Deemter plot of plate height against the mobile phase flow velocity according to Eq. (1). In the case illustrated, the parameters are: $A = 5$ μm, $B = 6$ mm^2/ms, $C = 5$ ms.

right hand side of Eq. (1) represents the contribution to the plate height from flow maldistribution in the packed column in the absence of extra-column effects. It is also called 'Eddy diffusion' term [23]. The second term stands for band spreading resulting from longitudinal diffusion of the sample component and in traditional column chromatography it contributes significantly to the plate height only at low flow velocities. The third term arises from mass transfer resistances [21–23] encountered by the sample components in the retention process based on their distribution between the mobile and stationary phases. According to the classical chromatographic theory [22,23], in columns packed with porous stationary phase particles the C parameter is largely determined by the slowness of intraparticle mass transfer and to some extent on that of film diffusion.

Eq. (1) is expected to hold reasonably well at mobile phase velocities not too much higher than the optimum value of u. The experiments were carried out in a relative narrow range of mobile phase velocity. For this reason any dependence of the A and C parameters on the flow velocity has been neglected [28,29]. A fundamental assumption underlying the present study is that Eq. (1) holds not only in HPLC with viscous flow, but also in CEC of neutral eluites. Our main intent is to compare the effect of the flow conditions on the parameters of Eq. (1). Employment of the same column with pressure-driven and voltage-driven mobile phase flow in the reversed-phase chromatography of low-molecular mass neutral sample components under otherwise identical conditions offers a unique opportunity to compare the effect of the two kinds of flow fields on the parameters of Eq. (1).

Another simple three-parameter equation for relating H to the mobile phase velocity is the Knox equation [30],

$$H = \frac{B}{u} + Au^{1/3} + Cu \qquad (2)$$

The physical meanings of the three terms of this equation are quite similar to the corresponding terms of Eq. (1), but in Eq. (2), the A term is velocity dependent. Parameters evaluated by Eqs. (1) and (2) for three different columns are compared in Table 1 and Fig. 2. In agreement with the literature [31], fitting both the μ-HPLC and CEC data obtained with a given column to Eq. (2) gives slightly higher A and lower C values than fitting to Eq. (1). Table 1 and Fig. 2 show that in the range of the experimental conditions, the corresponding parameters of Eqs. (1) and (2) obtained by μ-HPLC and CEC measurements with the same column do correlate very well.

Table 1
Comparison of van Deemter equation (Eq. (1)) and Knox's equation (Eq. (2)). The experimental conditions are listed in Fig. 2

Parameters	Benzaldehyde		*m*-Terphenyl	
	Slope	*r*	Slope	*r*
A	1.3	0.99	1.2	0.99
B	1.0	0.95	1.0	0.95
C	0.90	0.99	0.97	0.98

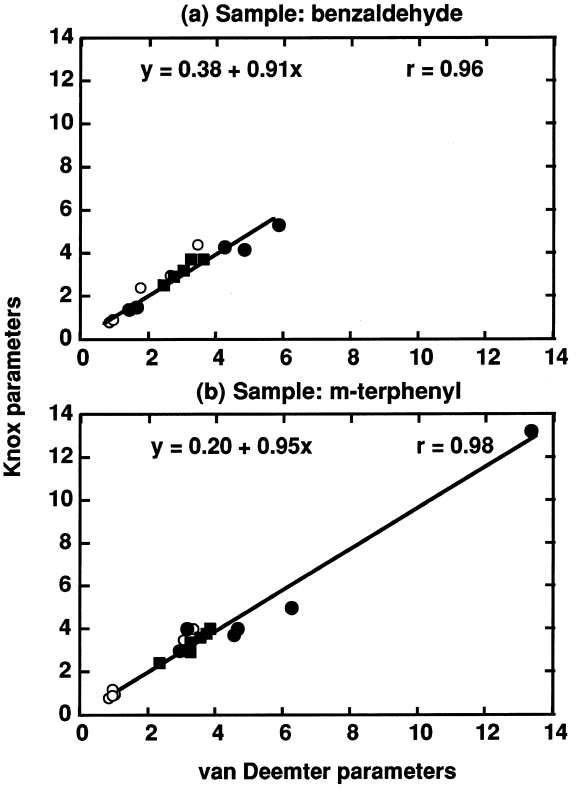

Fig. 2. Plots of van Deemter (Eq. (1)) parameters against Knox (Eq. (4)) parameters as measured in μ-HPLC and CEC modes with various columns under otherwise identical conditions. Columns and eluent are the same as Fig. 2. Samples, (a) benzaldehyde, (b) *m*-terphenyl; parameters, (○) A, (■) B, (●) C.

This finding justifies the use of the simpler van Deemter equation for evaluating the parameters. Before presenting the results we shall briefly examine the validity of the assumptions underlying this analysis.

3.1. Band spreading from sample introduction and Joule heating

Band spreading from other sources may have an untoward effect on column efficiency in μ-HPLC and CEC [1,32]. In our experiments, the time constant of on-column detection was less than 0.05 s so that the plate height contribution from detection was negligible [33–35].

When the sample enters the capillary column as a plug, the plate height contribution of sample injection, H_{inj}, in μ-HPLC was evaluated using the following relationship [32]

$$H_{inj} = \frac{\ell_{inj}^2}{12L} \quad (3)$$

where ℓ_{inj} is the length of the sample plug and L is the column length. The corresponding plate height increment due to electrokinetic injection in CEC is,

$$H_{inj} = \frac{(\mu E_{inj} t_{inj})^2}{12L} \quad (4)$$

where t_{inj} is the injection time, E_{inj} and μ are the actual electric field strength during injection and the electrophoretic mobility of the sample component respectively. The value of H_{inj} was calculated with the mobility of acrylamide obtained under a wide range of pertinent experimental conditions, and found to be less than 0.1 μm for both μ-HPLC and CEC. According to the results presented here, neither detection nor injection contributed significantly to band spreading in the μ-HPLC and CEC experiments.

Joule heating may also be the source of additional band spreading by virtue of radial temperature gradients [1,20,36] This was tested by examining the retention factors, k', of benzaldehyde, naphthalene, biphenyl, fluorene, and *m*-terphenyl from measurements in three columns packed with octadecylated silica gel in the applied voltage range from 1 to 30 kV. The results which are illustrated in Fig. 3 show

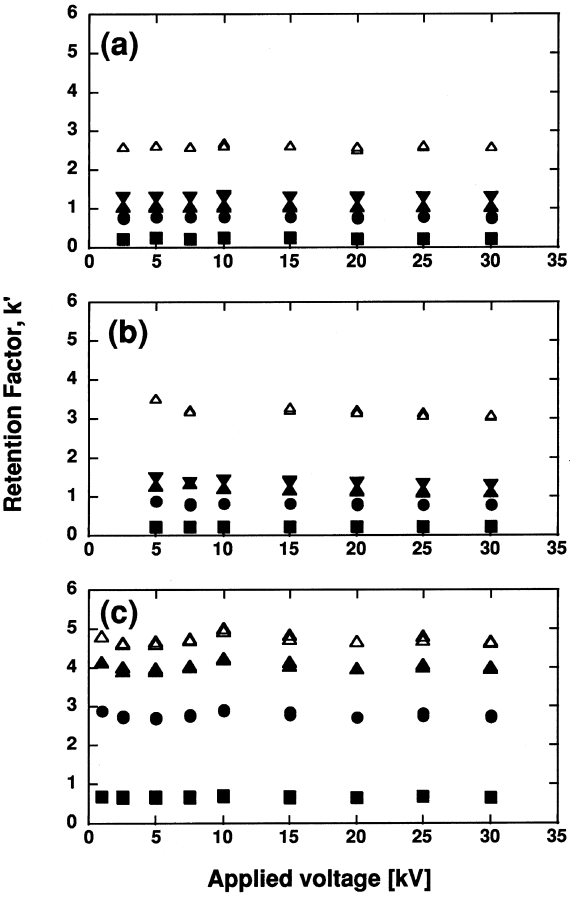

Fig. 3. Plots of the retention factor, k', against the applied voltage in the CEC mode. Columns, (a) 21/29 cm×50 μm capillary packed with 5 μm Spherisorb ODS 300 Å; (b) 23/31 cm×50 μm capillary packed with 6 μm Zorbax 300 Å; (c) 20/28 cm×50 μm capillary packed with 6 μm Zorbax 80 Å; eluent, 10 m*M* sodium-phosphate in water–acetonitrile mixture (2:3, v/v); sample components, (■) benzaldehyde, (●) naphthalene, (▲) biphenyl, (▼) fluorene, and (△) *m*-terphenyl. The temperature control of the forced air thermostat was set at 25°C for all experiments.

no decrease in the k' values upon increasing the applied voltage. Consequently, the effect of Joule heating on our CEC data has been neglected.

3.2. Reversed-phase chromatography

Both the μ-HPLC and CEC experiments were carried out under identical conditions typical in reversed-phase chromatography. The retention factors of a given sample component in CEC, k'_{CEC},

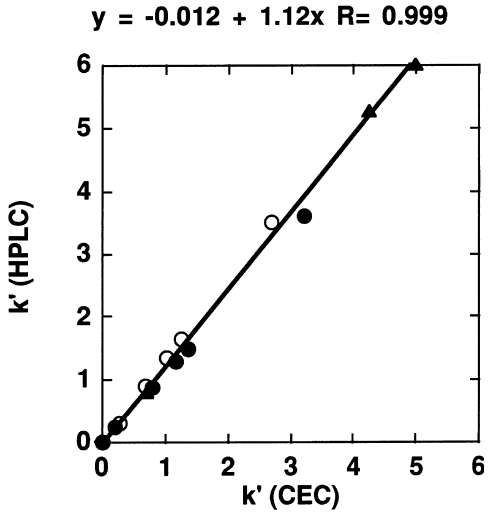

Fig. 4. Correlation between the retention factors measured in μ-HPLC and the CEC modes with various columns under otherwise identical conditions. Columns, (○) 21/29 cm×50 μm capillary packed with 5 μm Spherisorb ODS 300 Å; (●) 23/31 cm×50 μm capillary packed with 6 μm Zorbax 300 Å; (▲) 20/28 cm×50 μm capillary packed with 6 μm Zorbax 80 Å; eluent, 10 m*M* sodium-phosphate in water–acetonitrile mixture (2:3, v/v); sample components, benzaldehyde, biphenyl, fluorene, and *m*-terphenyl.

were plotted against k'_{HPLC}, the retention factor of the same sample component in μ-HPLC. In order to ascertain that the mechanism of retention is indeed the same in both μ-HPLC and CEC with the neutral small molecules of the sample mixture, the retention factors were measured under the same conditions but the nature of the flow. The close correlation ($r=$ 0.999) of the two sets of retention factors illustrated in Fig. 4 indicates that the migration velocities of the sample components were not affected by the strong electric field employed in the CEC experiments. We conclude that both the μ-HPLC and CEC systems represented bona fide reversed-phase chromatographic systems that differed only in the nature of the mobile phase flow.

4. Comparison of van Deemter parameters in μ-HPLC and CEC

In the absence of untoward kinetic phenomena, the chromatographic efficiency is largely determined by the flow field and the rate of diffusion of the sample components. We have been interested in comparing band spreading in several columns each operated with both viscous and electrosmotic flow under such experimental conditions that only the flow fields were different.

Direct comparison of column performance in μ-HPLC and CEC was made by separating polyaromatic hydrocarbons on several columns packed with three octadecylated-silica stationary phases commonly used in reversed-phase chromatography by using either pressure drop (μ-HPLC) or voltage drop (CEC) to drive the eluent across the column. The results are shown in Fig. 5 by plots of the data according to Eq. (1). Correlation coefficients for all plots were between 0.92 to 0.99. The corresponding chromatographic parameters, evaluated by using Eq. (1), are listed in Table 2. Variations in parameter *B* are negligible with respect to those in parameters *A* and *C*. The ratios of the *A* and *C* parameters measured in μ-HPLC over their value measured in CEC is called the attenuation factor which is also listed in Table 2. The *A*-term and *C*-term attenuation factors quantify the attenuation of band spreading, i.e. the reduction of the *A* and *C* terms in CEC with respect to their values in μ-HPLC.

The band spreading of an unretained tracer in columns packed with various octadecylated-silica particles or with siliceous and polymeric cation-exchanger particles of different pore sizes was also examined. The measurements were carried out at pH 7.0 when the stationary phases had fixed negative charges at the surface in addition to the hydrophobic functions. The pore size and the particle size of the stationary phases fell in the range of 80 Å to 1000 Å and of 5 to 8 μm, respectively. The results are presented in Table 3, and it is seen that except for the column packed with octadecylated-silica of 80 Å mean pore diameter, the *A* and *C* parameters were consistently higher with pressure driven (μ-HPLC) than with voltage driven (CEC) chromatography.

5. Flow maldistribution in packed columns

The anfractuous flow pattern in packed beds gives rise to band spreading due to spatial variations in flow velocity, i.e., maldistribution of the mobile

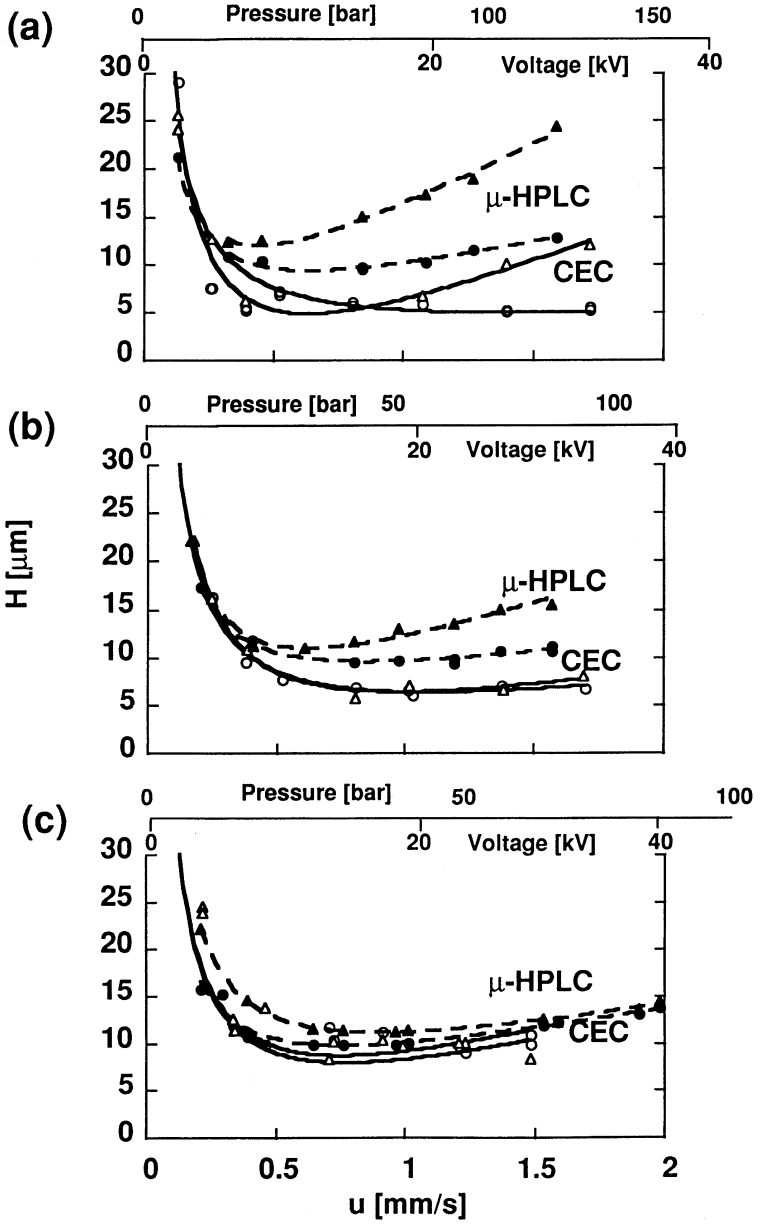

Fig. 5. van Deemter plots of data obtained with various packed capillary columns. Columns, (a) 21/29 cm×50 μm capillary packed with 5 μm Spherisorb ODS 300 Å; (b) 23/31 cm×50 μm capillary packed with 6 μm Zorbax ODS 300 Å; (c) 20/28 cm×50 μm capillary packed with 6 μm Zorbax ODS 80 Å. Measurements were carried out in both pressure (μ-HPLC) and voltage driven (CEC) modes under otherwise identical conditions; eluents, 10 m*M* sodium-phosphate, in water–acetonitrile mixture (2:3, v/v). Samples were (●,○) benzaldehyde and (▲,△) *m*-terphenyl, with the solid and open symbols representing pressure and voltage driven flows, respectively.

phase flow. As mentioned above, the plate height increment *A* in Eq. (1) measures the effect on band spreading due to the irregularity of the column packing and a large *A* value usually indicates that the column is poorly packed. The flow maldistribution is caused by inhomogeneity of the packing that results

Table 2
Mass transfer and column efficiency parameters of retained sample components evaluated in the μ-HPLC and CEC mode under otherwise identical conditions with three columns packed with octyldecylated silica. As suggested by the results in Fig. 5 the retention of the two neutral eluites, benzaldehyde and *m*-terphenyl is due to the same mechanism. Eluent, 10 m*M* sodium-phosphate in water–acetonitrile mixture (2:3, v/v). The attenuation factors were calculated by taking the ratio of the parameter values obtained with a given column under a given set of conditions. The parameters of any given chromatographic system were evaluated by Eq. (1)

PhaseSep ODS, particle diameter, 5 μm, pore size 300 Å (Column: 22/30 cm×50 μm)

Parameters	Benzaldehyde			*m*-Terphenyl		
	μ-HPLC ($k'=0.30$)	CEC ($k'=0.25$)	Attenuation factor	μ-HPLC ($k'=3.2$)	CEC ($k'=3.0$)	Attenuation factor
A (μm)	1.7	0.8	2.1	1.0	0.8	1.3
B (mm^2/ms)	2.4	3.0	NA	2.3	3.2	NA
C (ms)	6.0	1.4	4.2	13.3	4.6	2.9

Zorbax ODS, particle diameter, 6 μm, pore size 300 Å (Column: 23/31 cm×50 μm)

Parameters	Benzaldehyde			*m*-Terphenyl		
	μ-HPLC ($k'=0.23$)	CEC ($k'=0.20$)	Attenuation factor	μ-HPLC ($k'=3.6$)	CEC ($k'=3.2$)	Attenuation factor
A (μm)	3.4	0.9	3.8	3.3	0.9	3.7
B (mm^2/ms)	2.7	3.2	NA	3.2	3.5	NA
C (ms)	3.6	1.6	2.3	6.2	2.9	2.1

Zorbax ODS, particle diameter, 6 μm, pore size 80 Å (Column: 20/28 cm×50 μm)

Parameters	Benzaldehyde			*m*-Terphenyl		
	μ-HPLC ($k'=0.78$)	CEC ($k'=0.70$)	Attenuation factor	μ-HPLC ($k'=6.2$)	CEC ($k'=5.5$)	Attenuation factor
A (μm)	2.6	0.9	2.9	3.0	0.9	3.3
B (mm^2/ms)	2.7	3.6	NA	3.8	3.7	NA
C (ms)	4.8	4.2	1.1	4.5	3.1	1.5

Table 3
Mass transfer and column efficiency parameters of acrylamide, an unretained neutral marker evaluated in both the μ-HPLC and the CEC modalities under otherwise identical conditions with four columns. Eluent: 10 m*M* sodium-phosphate in water–acetonitrile mixture (2:3, v/v). The electrosmotic enhancement factors were estimated as the ratios of the two values of the same parameter in the μ-HPLC and the CEC mode

Column	*A* (μm)			*C* (ms)		
	μ-HPLC	CEC	Ratio	μ-HPLC	CEC	Ratio
Zorbax ODS, 6 μm/80 Å[a]	3.0	1.2	2.5	7.0	5.6	1.3
Zorbax ODS, 6 μm/300 Å[a]	3.0	1.0	3.0	4.5	2.8	1.6
PhaseSep ODS, 5 μm/300 Å[a]	1.2	0.5	2.4	6.1	1.4	4.4
PhaseSep SCX, 5 μm/300 Å[a]	1.0	0.5	2.0	6.0	1.8	3.3
PL-SCX, 8 μm/1000 Å[a]	4.0	1.0	4.0	12	2.2	5.5

[a] Particle diameter/pore diameter.

in stream splitting and velocity fluctuation. In the simplified version of the van Deemter equation the *A* term is expressed as

$$A = 2\lambda d_p \tag{5}$$

where d_p is the particle diameter and λ is a structural parameter of the column packing.

The A parameter is believed to be a weak function of velocity and in view of the particular flow field of EOF, we expect less band spreading from flow maldistribution in CEC than in μ-HPLC. By using a capillary bundle model [37], the mobile phase flow through a packed column is schematically illustrated in Fig. 6 with viscous flow and with EOF at the same pressure drop. In viscous flow through channels of different diameters the flow profiles are assumed to be close to parabolic and the mean flow velocities depend on the channel diameters as shown in Fig. 6a. This gives rise to band spreading although in reality mass exchange between the capillaries relaxes the maldistribution of flow as expounded by the 'coupling theory' [38]. According to von Smoluchowski [39], electrosmotic flow has a flat velocity profile and it is independent of the tube diameter when the double layer thickness is much smaller than the tube diameter. The idealized flow field with EOF is shown schematically in Fig. 6b. Comparison of Fig. 6a and 6b suggests that the magnitude of band spreading due to flow maldistribution ought to be smaller in CEC than in μ-HPLC under otherwise identical conditions. So far the details of the flow field in porous media under conditions of CEC are not yet well understood and the flow pattern is most likely a mixed viscous-electrosmotic flow.

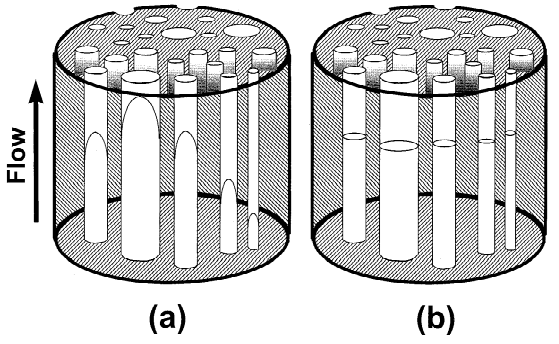

Fig. 6. Schematic illustration of the flow field in the capillary bundle model for packed bed with, (a) viscous flow, (b) electrosmotic flow. The maldistribution of viscous flow, which is responsible for the *A*-term in Eq. (1), is represented by capillaries of different diameters. Further bandspreading is caused by the parabolic flow profile in the capillaries. In CEC the electrosmotic flow velocity does not depend on the inner diameter of the cylindrical capillary tubing so that flow maldistribution is relaxed. Bandspreading is also attenuated by the flat flow profile in the capillaries.

The corresponding *A*-terms from μ-HPLC and CEC experiments with several columns were compared to quantify the change in the A term upon changing from viscous flow to electrosmotic flow. The graphs in Fig. 7 illustrate plots of parameter *A* measured with three different columns against the buffer concentration in both the μ-HPLC and the CEC experiments. In all cases, the value of the *A*-term was smaller in the CEC than in the μ-HPLC mode and the attenuation factor was in the range of two to four. Fig. 8 illustrates the dependence of the *A*-term attenuation factor on the retention factor. It is seen that the improvement in the value of the *A*-term is invariant at changing retention factor. The relatively small value of *A* in CEC is believed to arise from the relative insensitivity of the EOF velocity to the channel diameter and the results presented in Figs. 7 and 8 lend support to the schematic illustration in Fig. 6.

6. Intraparticle mass transfer resistances

According to the classical theory in HPLC with a well designed instrument and column, slowness of the diffusional mass transfer inside the stationary phase particles and the surrounding mobile phase is the main source of band spreading at high reduced velocities. The plate height increment, H_i, due to intraparticle mass transfer resistances for retained eluites has been expressed as [21,22,40],

$$H_i = \frac{\theta(k_o + k' + k_o k')^2 d_p}{30 k_o (1 + k_o)^2 (1 + k')^2} \cdot \frac{D_{eff}}{D_{app}} \cdot \frac{u d_p}{D_m} \tag{6}$$

where θ is tortuosity of the support, d_p is the particle diameter, D_m is the molecular diffusivity of the solute in the mobile phase, u is the interstitial mobile phase velocity, k' is the retention factor and

$$k_o = \frac{\epsilon_i (1 - \epsilon_e)}{\epsilon_e}$$

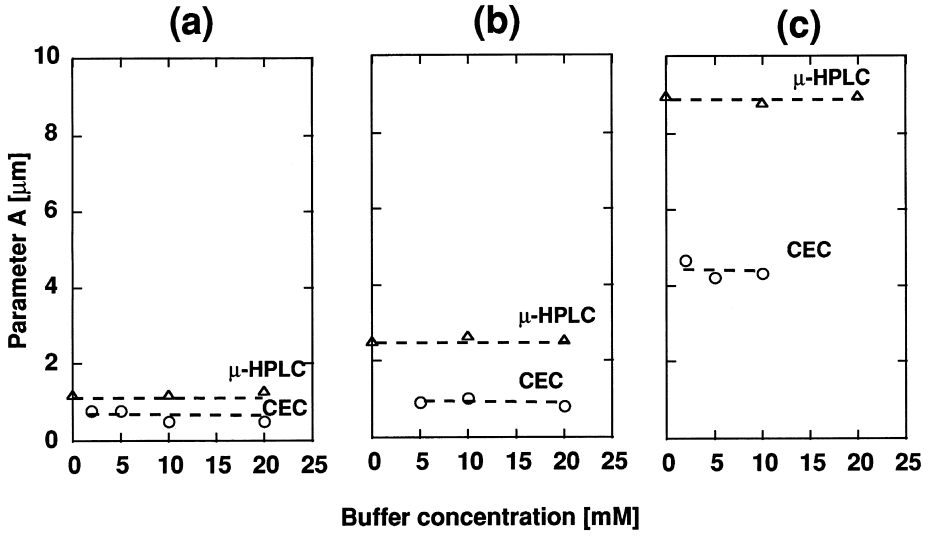

Fig. 7. Plots of parameter *A* against the buffer concentration in the μ-HPLC mode (△) and the CEC mode (○). Columns, (a) 21/29 cm×50 μm capillaries packed with 5 μm Spherisorb ODS 300 Å; (b) 26/34 cm×50 μm capillaries packed with 5 μm Spherisorb SCX 300 Å; (c) 34/42 cm×75 μm capillaries packed with 8 μm PL-SCX 1000 Å; eluents, (a) sodium-phosphate in water–acetonitrile mixture (1:1, v/v), (b–c) sodium-phosphate in water, pH 7.0.

where ϵ_i and ϵ_e are the intraparticulate and interstitial porosities, respectively. In a porous particle, D_{eff} is the effective molecular diffusivity in the pores of the packing [21,22,40] whereas D_{app} is the apparent diffusivity that accounts for transport in the porous particles by diffusion and by intraparticle convective transport. In pressure driven HPLC without pressure induced intraparticulate convection, $\frac{D_{eff}}{D_{app}} = 1$. In this paper, we assume that Eq. (6) holds not only in HPLC but also in CEC, where intraparticulate EOF may enhance the value of D_{app} with concomitant decrease in the mass transfer resistance. In this case, $\frac{D_{eff}}{D_{app}}$ is dependent on the electric driving force. By evaluating $H_i^{viscous}$ and H_i^{eo} from measurements by HPLC and CEC under the same conditions except the flow field, we can calculate the *C*-term attenuation factor $H_i^{viscous}/H_i^{eo}$ which is equal to $\frac{D_{app}}{D_{eff}}$. Eq. (6) can be viewed as a product of three factors: one expresses the structural properties of the porous particles, the other is the reciprocal *C*-term attenuation factor and the third is the reduced velocity, also called Peclet number.

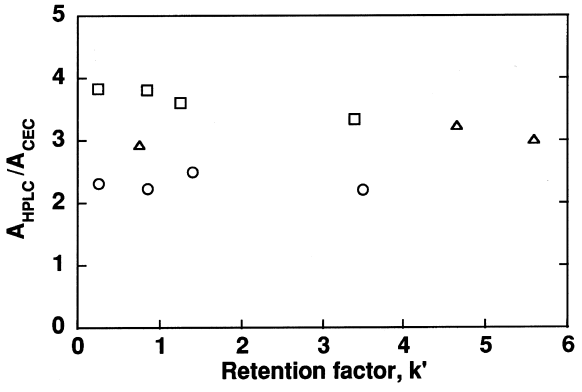

Fig. 8. Plot of the ratio A_{HPLC}/A_{CEC} against the retention factor, *k'*. Columns, (○) 22/30 cm×50 μm capillary packed with 5 μm Spherisorb ODS 300 Å; (□) 23/31 cm×50 μm capillary packed with 6 μm Zorbax ODS 300 Å, (△) 20/28 cm×50 μm capillary packed with 6 μm Zorbax ODS 300 Å; eluent, sodium-phosphate in water–acetonitrile mixture (2:3, v/v); samples, benzaldehyde, naphthalene, biphenyl, fluorene, *m*-terphenyl.

Fig. 9 schematically illustrates the intraparticle mass transport processes under conditions of traditional μ-HPLC and CEC. As shown in Fig. 9a, intraparticulate transport in μ-HPLC is by diffusion (D_{eff}) only except in the case of gigaporous supports where pressure induced intraparticulate convection may occur [40]. In CEC, it has been postulated

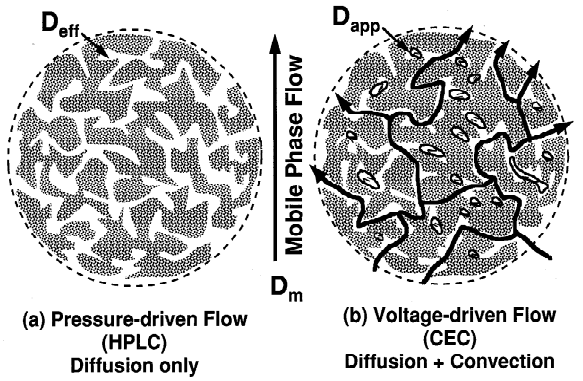

Fig. 9. Artist's rendition of intraparticle mass transfer with, (a) viscous flow, (b) electrosmotic flow. The slowness of mass transfer determines the magnitude of *C*-term in Eq. (1). In μ-HPLC, transport of solutes is by diffusion only while in CEC, intraparticle EOF augments transport between the interstitial fluid and the binding sites inside the porous particles by convection. The circulating patterns inside particle symbolize that even in dead-end pores EOF can enhance intraparticulate mass transport by convective mixing.

[18,40] that in porous supports with charged surface and sufficiently large pores, there may be a voltage induced intraparticulate convection, i.e. EOF, and the resulting convective transport relaxes mass transfer resistances and thus the magnitude of the C term. As shown in Fig. 9b, in addition to intraparticle EOF in interconnected pores, which facilitates transparticle convection, a recirculating EOF patterns may set up also in dead-end pores and thus intraparticle mass transport is further enhanced.

The data presented in Tables 2 and 3 lend strong support to the notion that mass transfer within the pores, i.e. the apparent diffusivity, is enhanced by intraparticle electrosmotic flow. With uncharged sample components, electrophoretic/electrosmotic effects are expected to be negligible. The observed reduction of mass transfer resistances in CEC and thus the effect of intraparticle electrosmotic flow on the band spreading is conveniently expressed by the corresponding *C*-term attenuation factor. Comparison of data in Tables 2 and 3 shows a significant reduction in the *C* parameter with stationary phases having 300 Å pores but not with the 80 Å pore size support. This difference is explained by overlap of the double layers within the narrow pores that precludes the development of electrosmotic intraparticle convection [41,42] inside the latter stationary phase particles. It is also seen from Table 3 that the *C* term is lower with the packings of 300 Å and 1000 Å pore size than with the narrow 80 Å pore size packing in CEC. This finding would indicate that intraparticulate electrosmotic convection can assist mass transfer inside the 300 Å pores at sufficiently high ionic strength so that gigaporous sorbents may not needed for high mass transfer rates at a price of reduced column loading capacity.

It is of interest that plots of the reduced plate height of column packed with gigaporous sorbents against the reduced velocity in HPLC and CEC, which are shown in Fig. 10, suggest that the intraparticle electrosmotic mixing in gigaporous column packings is much more effective in reducing the magnitude of the *C* term at a given reduced velocity than pressure induced intraparticle convection alias perfusion [40]. The plots based on literature data illustrate that the CEC data are flat even at relatively high reduced velocities and this augurs well for the development of rapid separations by pressure assisted CEC. Further, sufficiently strong intraparticle EOF should allow the use of relatively large (5–10 μm) particles, having adequately wide pores, to obtain high column efficiency in CEC and thus cast away the often perceived need of using 1 μm or smaller particles.

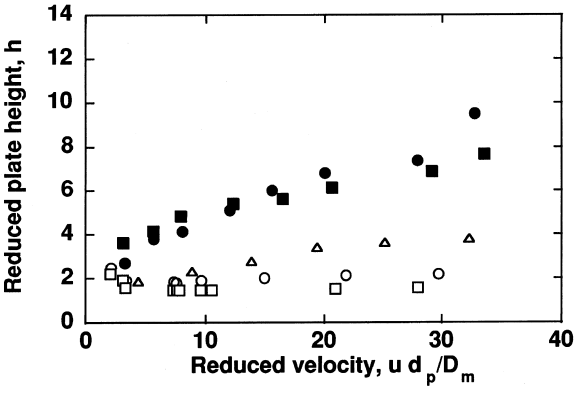

Fig. 10. Plots of the reduced plate height against the reduced velocity obtained from columns packed with gigaporous particles in both HPLC (solid symbols) and CEC (open symbols) modes. Data from the literature obtained with particles having the pore size stated, (△) 1000 Å [7], (○) 1000 Å [18], (●) 1000 Å [40], (□) 4000 Å [18], (■) 4000 Å [40].

6.1. Retention factor

The effect of the retention factor on band spreading in CEC with packed capillary columns has also been investigated and the results are presented in Fig. 11. A theoretical *C*-term attenuation factor was calculated for a cylindrical open tube with retentive innerwall from the *C* terms with viscous flow ($C_{\text{parabolic}}$) and with electrosmotic flow (C_{flat}) [23] as,

$$\frac{C_{\text{para}}}{C_{\text{flat}}} = \frac{6\alpha^2 - 16\alpha + 11}{6(1-\alpha)^2} \tag{7}$$

where $\alpha = 1/(1+k')$.

In Fig. 11 the dependence of this theoretical *C* term attenuation factor on the retention factor is illustrated. Whereas the comparison of theoretical and experimental results in Fig. 11 is a very crude one, it shows that the attenuation of the mass transfer resistances upon replacing viscous flow by electrosmotic flow is significant when the retention factor is small ($k' < 1$). Indeed, Bruin et al. [43] had showed that the plate efficiency in voltage driven open tubular chromatography was higher than that in pressure driven open tubular liquid chromatography by a factor of about two, as measured by the ratio of the mobile phase mass transfer terms. Such a behavior is often predicted when the main source of band spreading rests with the mobile phase.

The moderate low band spreading with electrosmotic flow may be exploited in open tubular capillary electrochromatography to enhance efficiency. The employment of capillaries with a porous stationary phase layer at the innerwall (PLOT columns) appears particularly attractive due to the relatively high loading capacity of PLOT columns [44].

6.2. Temperature

The speed of chromatographic separation can be increased by increasing the temperature and thus enhance the transport properties, such as diffusivity and fluidity. In order to explore the effect of elevated temperatures in CEC a set of experiments was carried out with a capillary column packed with 5 μm 300 Å Spherisorb ODS particles. All sample components were neutral aromatic hydrocarbons not subject to electrophoretic migration. The EOF velocity was measured by using acrylamide as the inert tracer. The retention factors were evaluated at column temperatures ranging from 20 to 60°C and the data were plotted in Fig. 12. The resulting linear van't Hoff plots and the retention enthalpies, ΔH°, calculated from the slopes, are also shown. The dependence of the plate efficiency measured with the

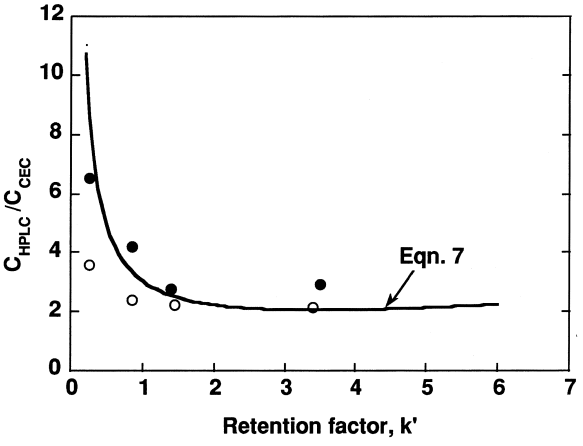

Fig. 11. Dependence of the ratio $C_{\text{HPLC}}/C_{\text{CEC}}$ on the retention factor, k'. The solid line is drawn according to Eq. (7) and the data points were measured as follows. The columns and eluents are the same as Fig. 4.

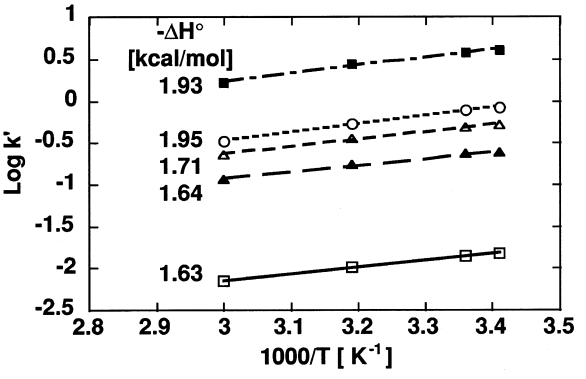

Fig. 12. Plot of the logarithmic retention factors against the reciprocal absolute temperature. Column, 21/29 cm×50 μm capillary packed with 5 μm Spherisorb ODS 300 Å; eluent, 10 m*M* sodium-phosphate in water–acetonitrile mixture (2:3, v/v); samples, (●) acrylamide, (□) benzaldehyde, (▲) naphthalene, (△) biphenyl, (○) fluorene, and (■) *m*-terphenyl.

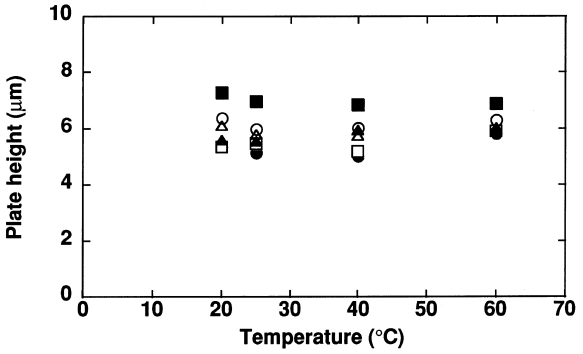

Fig. 13. Plots of the plate height against temperature. The column and experimental conditions are the same as Fig. 12.

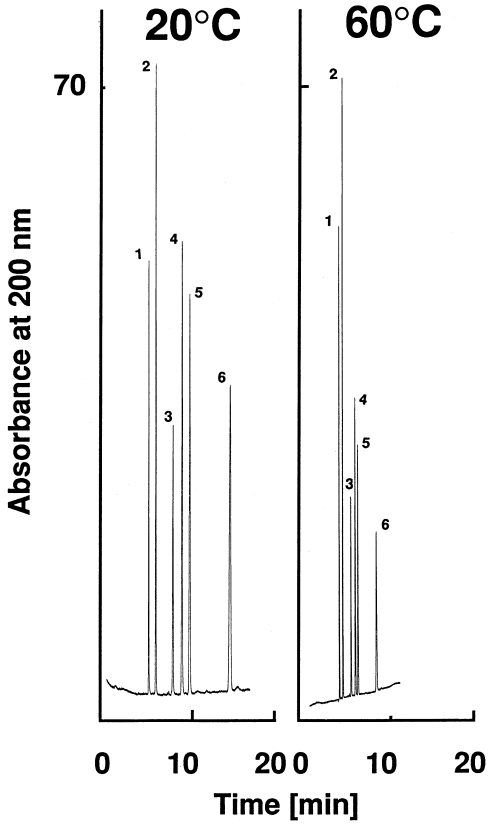

Fig. 14. Electrochromatograms of polycyclic aromatic hydrocarbons obtained at 20 and 60°C. Column, 21/29 cm×50 μm capillary packed with 5 μm Spherisorb ODS 300 Å; eluent, 10 m*M* sodium-phosphate in water–acetonitrile mixture (2:3, v/v) applied voltage, 20 kV; samples, (1) acrylamide, (2) benzaldehyde, (3) naphthalene, (4) biphenyl, (5) fluorene, and (6) *m*-terphenyl.

aromatic hydrocarbons on the temperature is illustrated in Fig. 13. Since the reduced plate heights are about unity over the whole temperature range, elevation of column temperature from 20 to 60°C may not suffice to bring about a significant improvement in the plate efficiency. None the less the speed of separation by the CEC system at hand can be significantly increased by raising the temperature from 20° to 60°C. This is seen from the comparison of the two chromatograms in Fig. 14 and as can be inferred from the plots of the EOF velocity against the temperature shown in Fig. 15. It is seen that the EOF increases with the temperature and this effect is attributed mainly to a decrease in the viscosity with increasing temperature. As a rule of thumb the decrease is about 2% per 1°C under conditions similar to those in Fig. 15.

6.3. Buffer Concentration

In light of von Smoluchowski's equation, the magnitude of the intraparticle electrosmotic flow is expected to change with the buffer composition. The *C*-term in Eq. (1) measures the magnitude of mass transfer resistances associated with the transport of the sample component of interest to the stationary phase surface [21–23] in the extra- and intraparticulate space. In the following we report the results of a set of experiments carried out in both μ-HPLC and CEC modes in which the concentration of the buffer changes. Three columns packed with the following stationary phases were used in these experiments:

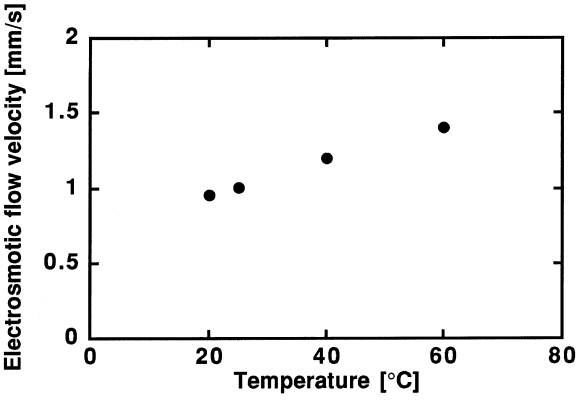

Fig. 15. Plot of electrosmotic flow velocity against temperature. The column and eluent conditions are the same as Fig. 12.

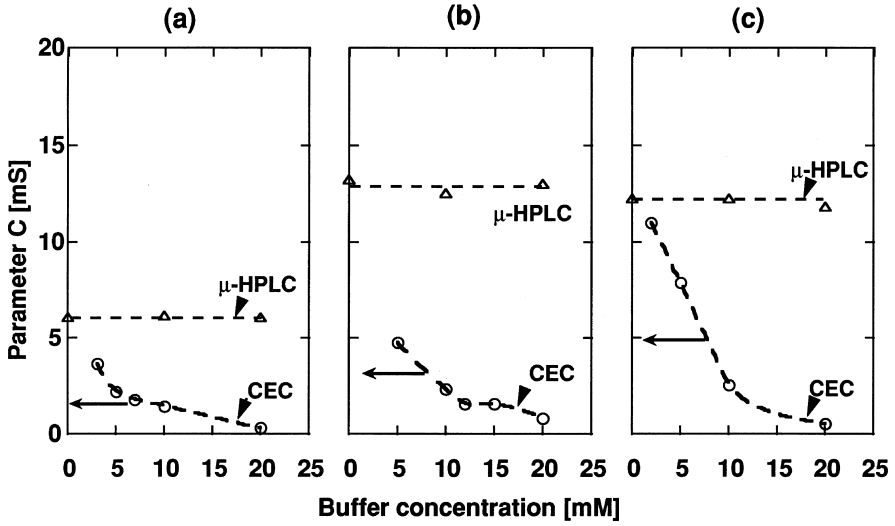

Fig. 16. Plots of parameter *C* against the buffer concentration as evaluated from the migration rate of acrylamide in the μ-HPLC mode (△) and the CEC mode (○). The columns and eluents are the same as Fig. 7.

300 Å siliceous ODS, 300 Å siliceous SCX and 1000 Å polymeric SCX. The observed variations in the intraparticle mass transfer resistances are shown in Fig. 16 as a function of buffer concentration for both μ-HPLC and CEC. In μ-HPLC the buffer concentration has shown no effect on the intraparticulate mass transfer in the concentration range investigated as expected in the reversed-phase liquid chromatography of nonpolar substances. In CEC, the intraparticulate mass transfer resistances were seen to increase and approach the value in μ-HPLC with decreasing buffer concentration. This is attributed to the increasing double layer thickness [39,41]. Hence it seems to be advantageous to employ relatively high buffer concentration in CEC with mesoporous sorbents.

In order to examine the effect of relatively high buffer concentration, experiments were carried out at

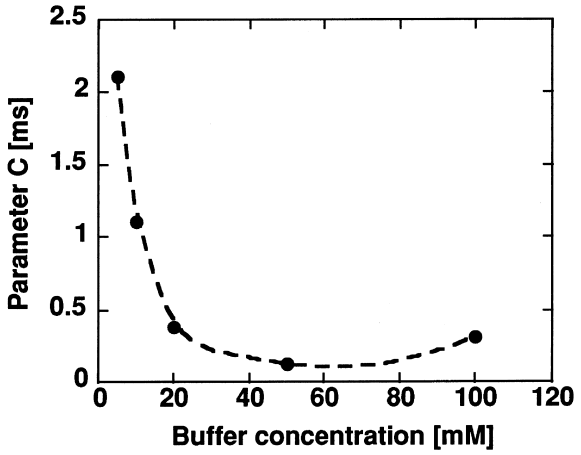

Fig. 17. Plot of parameter C against the buffer concentration as evaluated from the migration rate of acrylamide in the CEC mode. Column, 25/33 cm×50 μm capillary packed with 5 μm Spherisorb SCX 300 Å; eluent, sodium-phosphate, pH 7.0; tracer, acrylamide.

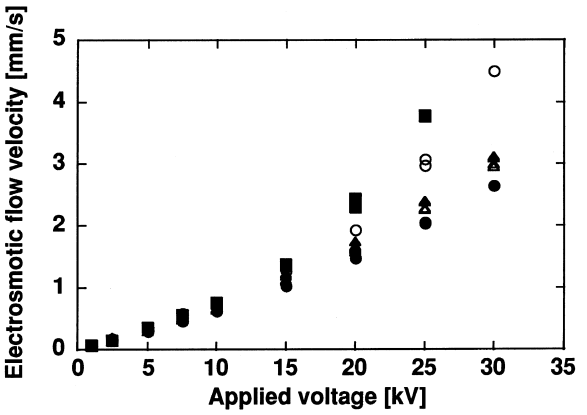

Fig. 18. Plot of the electrosmotic flow velocity against the applied voltage with the buffer concentration as the parameter. The column and sample are the same as Fig. 17; eluent, (△) 5, (●) 10, (▲) 20, (○) 50, (■) 100 m*M* sodium-phosphate, pH 7.0.

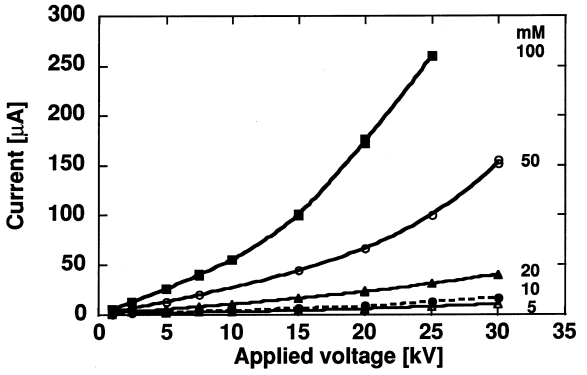

Fig. 19. Plot of the current against the applied voltage with the buffer concentration as the parameter. The column and sample are the same as Fig. 17; eluent, (△) 5, (●) 10, (▲) 20, (○) 50, (■) 100 m*M* sodium-phosphate, pH 7.0.

buffer concentrations as high as 100 m*M* phosphate. The column was packed with Spherisorb SCX particles, pore size 300 Å. The results are illustrated in Fig. 17 by a plot of the *C* parameter in CEC against the buffer concentration. The result was unexpected not only because the plot showed a minimum at 60 m*M* buffer concentration but also for the only slight increase in the *C* parameter when the buffer concentration was raised from 40 to 100 m*M*. As shown in Fig. 18, the electrosmotic flow velocity increased in a nonlinear fashion at applied voltages greater than 15 kV. This behavior was most likely caused by Joule heating at high buffer concentration and in high electric field as illustrated by plots of the current against the applied voltage shown in Fig. 19. With the high electrosmotic flow velocity, one can foresee the combined use of high buffer concentration and applied voltage to achieve rapid separations.

7. Conclusions

The results of this study confirm that under otherwise identical conditions the magnitude of band spreading is smaller in a given chromatographic column when the mobile phase is driven by voltage (EOF) rather than by pressure (viscous flow). With voltage driven flow, the *A* and *C* parameters of the simplified van Deemter equation are approximately two to four times lower than with pressure driven flow. This accounts for the observation that the plate efficiency is higher in CEC than in μ-HPLC. In the practice of CEC the flow field appears to reflect features of both electrosmotic and viscous flow. Its detailed mapping will require elaborate computer simulation.

The EOF velocity in any given CEC column and thus the maximum speed of separation is limited by the maximum permissible applied voltage. Experimental results presented here strongly suggest that intraparticle mass transfer is enhanced by intraparticle EOF. Consequently, the interstitial mobile phase velocity and thus the speed of separation, could be increased by employment of additional viscous flow, i.e. pumping, with a rather modest loss of column efficiency. This means that the criticism about the poor flow control in CEC could be refuted by using pressure assisted CEC without much loss of efficiency but with a large gain in the speed of analysis. The notion of pressure assisted CEC has been put forward many years ago [15,16,45]. It should be noted that the early work on this subject was aimed at the enhancement of the selectivity of the hybrid electrochromatographic system. On the other hand, the present argument calls for a speeding up the separation by employing a dual driving force for the mobile phase. This would overcome the limitations of EOF due to the constraints on the applied voltage and would reduce the time of separation.

So far most applications of CEC targeted the separation of small neutral and usually hydrophobic molecules by reversed-phase chromatography. When the sample components to be separated carry different charges, the separation processes may be much more complicated than with the neutral molecules. Ionized migrants, often large molecules, may be subject to additional electrophoretic band spreading and band distortion. On the other hand, focusing due to the interplay of electrophoretic and chromatographic forces may result in peaks much sharper than the chromatographic model used here would predict [2]. The mechanism of separation by CEC may be even more complicated when the migration of ionized sample components is counterdirectional to EOF as shown by isocratic separation of basic proteins

and peptides by CEC on a positively charged chromatographic surface [44]

Practical considerations strongly suggest that CEC will benefit from the development of new types of chromatographic columns having different architectures, such as porous layer open tubular (PLOT) and packed monolithic columns. PLOT columns, which have porous stationary phase annulus at the column inner wall, have the advantages of providing high permeability and good column efficiency. Such columns can often be employed in commercial instruments designed for CZE without untoward bubble formation. The most promising column architecture for CEC applications is expected to emerge from the further development of monolithic columns. The concept of forming in situ a porous monolith for column packing is particularly applicable to capillary columns due to their small lumen which does not allow the formation of temperature or other gradients that would lead to nonuniform structure. Monolithic column packing eliminates the need for retaining frits which are notoriously the weakest points of CEC columns. The often poor stability of conventionally packed CEC columns is due to the migratory propensity of charged packing particles under high electric field.

Acknowledgements

E.W. is a recipient of a Merck Fellowship. This work was supported by Grant No. GM 20933 from the National Institute of Health, US Department of Health and Human Resources. Our particular thanks to Dell Farnan for assistance in the μ-HPLC experiments. We thank Frank Warner of Polymer Laboratories Ltd. for supplying the gigaporous styrenic stationary phases, Jack Kirkland of Hewlett Packard for supplying the Zorbax particles, and Peter Myers of Phase Separations Co. for supplying the Spherisorb particles used in this study.

References

[1] J.H. Knox, J. Chromatogr. A 680 (1994) 3.
[2] N.W. Smith, M.B. Evans, Chromatographia 38 (1994) 649.
[3] R.J. Boughtflower, T. Underwood, J. Maddin, Chromatographia 41 (1995) 398.
[4] M.M. Dittmann, K. Wienand, F. Bek, G.P. Rozing, LC·GC 13 (1995) 800.
[5] J.H. Knox, I.H. Grant, Chromatographia 32 (1991) 317.
[6] M.M. Dittmann, G.P. Rozing, J. Chromatogr. A 744 (1996) 63.
[7] G. Choudhary, Cs. Horváth, J. Chromatogr. A 781 (1997) 161.
[8] A.S. Rathore, Cs. Horváth, J. Chromatogr. A 781 (1997) 185.
[9] B. Behnke, E. Grom, E. Bayer, J. Chromatogr. A 716 (1995) 207.
[10] F. Leliévre, C. Yan, R.N. Zare, P. Gareil, J. Chromatogr. A 723 (1996) 145.
[11] C. Yan, R. Dadoo, R.N. Zare, D.J. Rakestraw, D.S. Anex, Anal. Chem. 68 (1996) 2726.
[12] P. Sandra, A. Dermaux, V. Ferraz, M.M. Dittmann, G. Rozing, J. Microcol. Sep. 9 (1997) 409.
[13] R. Dadoo, R.N. Zare, C. Yan, D.S. Anex, Anal. Chem. 70 (1998) 4787.
[14] J.H. Knox, I.H. Grant, Chromatographia 24 (1987) 135.
[15] T. Tsuda, Anal. Chem. 60 (1988) 1677.
[16] V. Pretorius, B.J. Hopkins, J.D. Schieke, J. Chromatogr. 99 (1974) 23.
[17] R. Asiaie, X. Huang, D. Farnan, Cs. Horváth, J. Chromatogr. A 806 (1998) 251.
[18] D. Li, V.T. Remcho, J. Microcol. Sep 9 (1997) 389.
[19] J.J. van Deemter, F.J. Zuiderweg, A. Klinkengberg, Chem. Eng. Sci. 5 (1956) 271.
[20] J.H. Knox, Chromatographia 26 (1988) 328.
[21] Cs. Horváth, H.J. Lin, J. Chromatogr. 126 (1976) 401.
[22] Cs. Horváth, H.J. Lin, J. Chromatogr. 149 (1978) 43.
[23] J.C. Giddings, Dynamics of Chromatography, Marcel Dekker, New York, 1965, 48.
[24] B.L. Karger, L.R. Snyder, Cs. Horváth, An Introduction To Separation Science, John Wiley, New York, 1973, 135.
[25] Cs. Horváth, W.R. Melander, in: E. Heftmann (Ed.), Chromatography, Elsevier, Amsterdam, 1983, p. A27.
[26] J.C. Giddings, J. Chromatogr. 5 (1961) 61.
[27] J.H. Knox, J. Chromatogr. A 831 (1999) 3.
[28] A. Klinkenberg, Anal. Chem. 38 (1966) 489.
[29] A. Klinkenberg, Anal. Chem. 38 (1966) 491.
[30] P.A. Bristow, J.H. Knox, Chromatographia 10 (1977) 279.
[31] E. Katz, K.L. Ogan, R.P.W. Scott, J.Chromatogr. 270 (1983) 51.
[32] J.C. Sternberg, Adv. Chromatogr. (1966) 205.
[33] H. Rebscher, U. Pyell, Chromatographia 38 (1994) 737.
[34] U. Pyell, H. Rebscher, A. Banholczer, J. Chromatogr. A 779 (1997) 155.
[35] Y. Zhang, W. Shi, L. Zhang, H. Zou, J. Chromatogr. A 802 (1998) 59.
[36] N.M. Djordjevic, P.W. Fowler, F. Houdiere, G. Lerch, J. Liq. Chromatogr. Rel. Technol. 21 (1998) 2219.
[37] J. Bear, Dynamics of Fluids in Porous Media, Dover Publications, New York, 1988, 152.

[38] J.C. Giddings, Anal. Chem. 35 (1963) 2215.
[39] M. von Smoluchowski, Bull. Int. Acad. Sci. Cracovie, (1903) 184.
[40] D. Frey, E. Schweinheim, Cs. Horváth, Biotechnol. Prog. 9 (1993) 273.
[41] C.L. Rice, R. Whitehead, J. Phy. Chem. 69 (1965) 4017.
[42] Q.H. Wan, Anal. Chem. 69 (1997) 361.
[43] G.J.M. Bruin, P.P.H. Tock, J.C. Kraak, H. Poppe, J. Chromatogr. 517 (1990) 557.
[44] X. Huang, J. Zhang, Cs. Horváth, J. Chromatogr. A, (1999), in press.
[45] S. Kitagawa, T.A.H. Watanabe, M. Nakashima, T. Tsuda, J. Microcol. Sep. 9 (1997) 347.